THEORETICAL STUDIES OF THERMAL DECOMPOSITION OF ANHYDROUS CADMIUM AND SILVER OXALATES
Part I. Electronic structure calculations

A. Koleżyński and A. Małecki[*]

AGH University of Science and Technology, Faculty of Materials Science and Ceramics, Al. Mickiewicza 30
30-059 Cracow, Poland

The results of first principles calculations of band structure, density of states and electron density topology of CdC_2O_4 and $Ag_2C_2O_4$ crystals are presented. The calculations have been performed with WIEN2k ab initio program, using highly precise full potential linearized augmented plane wave (FP LAPW) method within Density Functional Theory formalism. The obtained SCF electron density has been used in calculations of Bader's AIM (atoms in molecules) topological properties of the electron density in crystal. The obtained results show important similarities in electronic structure and electron density topology of both compounds and allow supposing, that during the thermal decomposition process these compounds should behave similarly, which is in agreement with the experiment.

Keywords: *electron density topology, FP LAPW ab initio calculations, thermal decomposition*

Introduction

Many of known anhydrous metal oxalates MC_2O_4 (M is Fe, Co, Ni, Zn, Cu – Kondrashev *et al*. [1]; Cd – Jeanneau *et al*. [2]) are obtained from thermal decomposition of the related hydrates (Naumov *et al*. [3], Małecka *et al*. [4, 5],) and belong to the isostructural family of anhydrous oxalates β-MC_2O_4 with monoclinic unit cell P2$_1$/*n*, with similar cell parameters, arrangement of the MO$_6$. octahedra and oxalate anions, but different ways of thermal decomposition leading to *i*) Me+2CO$_2$, *ii*) MeO+CO+CO$_2$ or *iii*) MeCO$_3$+CO and then to MeO+CO+CO$_2$ [6–13]. There is still lack of consistent description and explanation of the origin and thermal decomposition path (to metal, metal oxide, or metal carbonate) in given oxalate. Moreover, there are no published results (at least we have found none) of ab initio calculations for mentioned above materials. Recent advances in solid state methods, together with rapid development in computer power, allow despite the low symmetry of these compounds, to perform such calculations even using recent personal computers. One can expect, that such calculations will give some insight into the thermal decomposition process and should allow after analysis of the electronic properties of different anhydrous oxalates, not only to explain the experimental data but also to predict the properties and decomposition paths for the other compounds. In this paper we present the results of calculations undertaken for two compounds (cadmium and silver oxalates) showing similar thermal decomposition paths i.e. to metal and carbon dioxide. The paper consists of two part – in the first one we present the results of the ab initio electronic structure calculations and in the second the detailed analysis of obtained results, with calculated bond orders and valences from the point of view of the thermal decomposition process.

Computational details

The first principle calculations of the band structure, density of states and electron density topology of CdC_2O_4 and $Ag_2C_2O_4$ crystals have been performed with WIEN2k ab initio program [14], using highly precise full potential linearized augmented plane wave (FP LAPW) method within density functional theory (DFT) formalism [15–20]. The 500 *k*-points (7×8×7 and 13×7×4 mesh within the irreducible Brillouin zone for cadmium and silver oxalates, respectively) and Rk_{max} parameter (which controls the size of the basis sets) equal to 7.5 and GGA-PBE exchange-correlation potential [21], have been chosen for calculations. This gives well converged basis sets consisting of over 5000 LAPW functions plus local orbitals (added for consistent treatment of semicore and valence states in one energy window, hence ensuring proper orthogonality). The following values of muffin-tin radii (R_i) for both structures were used [a.u.]: Cd, Ag – 1.8, O – 1.16, C – 1.16. The following convergence criteria for SCF calculations $\Delta E_{SCF} \leq 10^{-5}$ Ry for total

---

energy and $\Delta\rho_{SCF} \leq 10^{-5}$ e for electron density topology analysis were chosen. The band structure was calculated for selected high symmetry points defined for monoclinic unit cell (Group no. 14 on Bilbao Crystallographic Server http://www.cryst.ehu.es).

The electron density distribution in crystal cell, obtained from self-consistent calculations, was used for Bader's AIM method (atoms in molecules), which allows to analyze topological properties of electron density. The main idea of this method is based on the theorem, that one can divide crystal volume, to well defined areas assigned to particular atoms (atom basins), separated by surfaces, defined by equation $\nabla\rho(r)n(r)=0$ for every point r in crystal, where $n(r)$ – vector normal to the surface. In this way one can define 'atoms' in the crystal, but what's more, Bader showed, that such partitioning give us a vector field of the gradient of scalar electron density, where every field line starts and ends in one of electron density critical points (extremum, where the condition $\nabla\rho(r)=0$ is fulfilled). In three dimensional space, there are possible only four different types of critical points, defined usually by a pair (rank, signature), where rank is a number of nonzero eigenvalues of electron density Hessian matrix calculated for critical point and signature is an algebraic sum of the signs of these eigenvalues (number of positive curvatures minus number of negative curvatures in three orthogonal directions). One have then the following critical points: attractor $(3, -3)$ – atomic core, repellor $(3, 3)$ – cage critical point and saddle points: $(3, 1)$ ring critical point and $(3, -1)$ bond critical point.

Bader pointed out, that chemical bond can be analyzed by means of the electron density topology and bond path is a line of maximum density connecting bond critical point BCP $(3,-1)$ with two attractors $(3,-3)$. The Laplacian of electron density $\nabla^2\rho(r)$, defined as a trace of the Hessian matrix (sum of diagonal elements) represents the local charge concentration, providing a mapping of the electron pairs of the Lewis and VSEPR models and recovers the shell structure of an atom by displaying a corr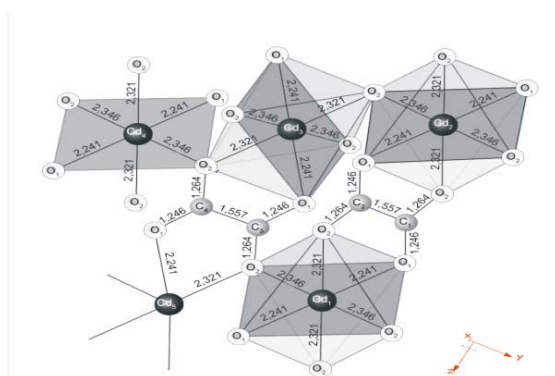esponding number of alternating shells of charge concentration and charge depletion. The properties of critical points give us many additional information about the global crystal properties.

Cadmium oxalate structure

Cadmium oxalate can be described as layered material (Fig. 1), formed by cationic layers built from corner-shared CdO_6 octahedra, linked together via bidentate chelating oxalate groups [2]. Cadmium polyhedron, include six oxygen atoms, all belonging to oxalate groups and is nearly regular octahedron, with three different Cd–O bond lengths (2.241, 2.321 and 2.346 Å). The oxalate group is nearly planar, with mean atomic deviation of 0.002 Å from the plane. Crystal structure parameters and fractional atomic coordinates, used in ab initio calculations are listed in Table 1.

Silver oxalate structure

Anhydrous silver oxalate has monoclinic unit cell $P2_1/_c$ (Naumov *et al.* [22]). Oxalate anions (each one is coordinated to six Ag^+ cations) form a framework with the layers in the (200) planes and the channels extended along [100] with Ag–Ag dimers located inside these channels. Each silver atom is coordinated to four oxygen atoms of three oxalate anions (flatten tetrahedron) and another silver atom (Fig. 2). Respective crystal structure parameters and fractional atomic coordinates used in calculations are listed in Table 1.

One can easily see the similarities of both structures: the carbon–carbon bonds are about 1.6 Å long close to the average C–C distance in carbonate and the metal–oxygen bonds are of similar length and oxalate anions are well defined in the structure.
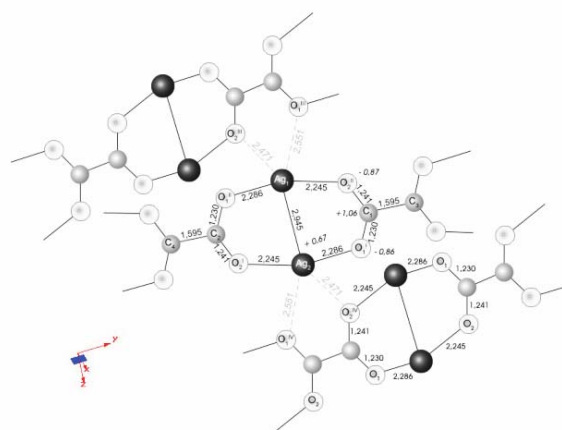

Fig. 2 $Ag_2C_2O_4$ crystal structure

Fig. 1 CdC_2O_4 crystal structure

Table 1 Anhydrous cadmium and silver oxalates crystal data and fractional atomic coordinates (structure data for cadmium and silver oxalates taken from [2, 19], respectively)

Structure	Space group	a/Å	b/Å	c/Å	β/°	V/Å^3
CdC$_2$O$_4$	P2$_1$/n	5.826	5.252	5.832	113.86	163.19
Ag$_2$C$_2$O$_4$	P2$_1$/c	3.4603	6.1972	9.548	103.47	199.12

Fractional atomic coordinates

Structure	Atom symbol	X	y	z
CdC$_2$O$_4$	Cd	0	0	0
	O$_1$	0.8893	0.2305	0.2625
	O$_2$	0.8214	0.1954	0.6104
	C	0.9168	0.1218	0.4619
Ag$_2$C$_2$O$_4$	Ag	0.1416	0.49443	0.15782
	O$_1$	0.507	0.7859	0.1183
	O$_2$	0.175	0.8228	0.8903
	C	0.403	0.884	0.0037
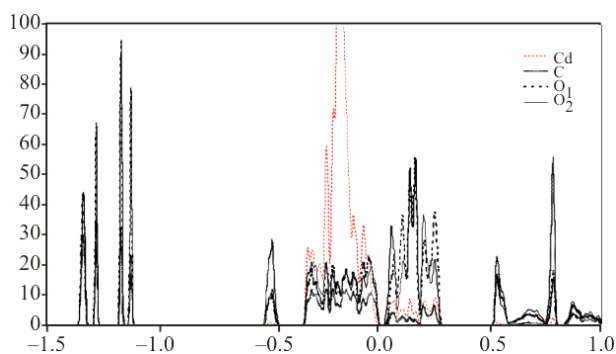
Fig. 3 Total density of states calculated for cadmium oxalate (only total DOS for individual atoms are shown in the picture)
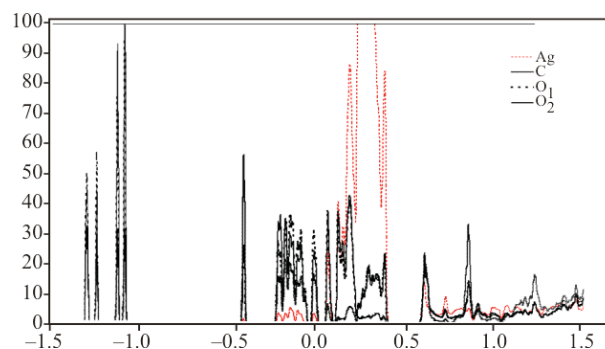
Fig. 4 Total density of states calculated for silver oxalate (only total DOS for individual atoms are shown in the picture)

Results and discussion

In spite of different chemical composition, both oxalates have similar crystal structure (monoclinic unit cell) and the behavior during thermal decomposition (both decompose to metal and carbon dioxide). As a consequence, one can predict similar qualitative picture of the band structure and density of states for these oxalates. Of course there should be also differences due to doubled number of silver in crystal cell comparing to number of cadmium atoms (cadmium oxalate: 52 valence bands, E_F=0.26882 Ry, band gap 0.246 Ry; silver oxalate: 70 valence bands, E_F=0.39104 Ry, band gap 0.181 Ry). Figures 3 and 4 show the total densities of states for the individual atoms in cadmium and silver oxalates crystals, respectively. The DOS-es are quite similar: in valence region there are three sharp peaks. The carbon 2s and 2p electrons are mixed with oxygen 2s electrons in two peaks (carbon 2s electrons at about –1.3 Ry and 2p electrons at about –1.1 Ry). The next peak at about

–0.5 Ry consists of 2s and 2p electrons from carbon and oxygen. One can see also two broader regions with filled states up to Fermi level. The first one broader, built up from the electron density originated from metal cations (d electrons), mixed in both cases with the oxygen 2p electrons; the second one little narrower containing mostly the oxygen 2p electrons, mixed with small amount of carbon 2p and metal d electrons. In conduction region there are mainly mixed states of oxygen 2p, carbon 2p and metal s electrons. One should notice however that the shapes of total DOS-es for cadmium and silver in valence region are quite different: In case of silver, most of electrons states are located close to Fermi level and much smaller number of states in slightly lower energies range. For cadmium the regions with big and small number of states are reversed: close to Fermi level there is smaller DOS than for lower energies. Nevertheless in both cases total DOS for cadmium and silver in valence region are similarly diffuse (about 0.65 Ry wide), close to Fermi level and mixed with only
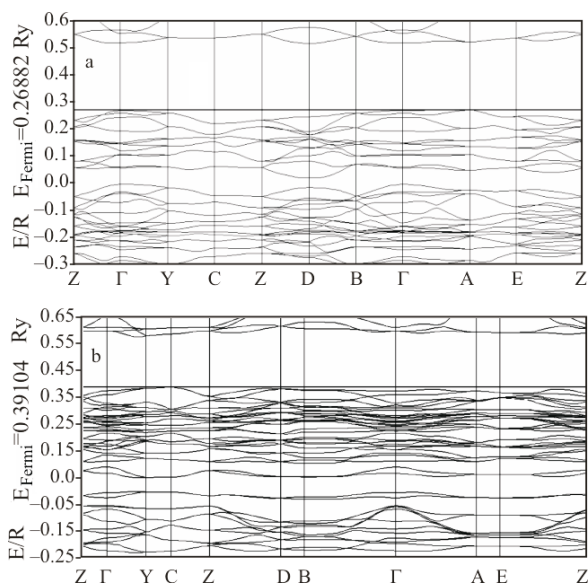
Fig. 5 Band structures calculated for a – cadmium and
b – silver oxalates
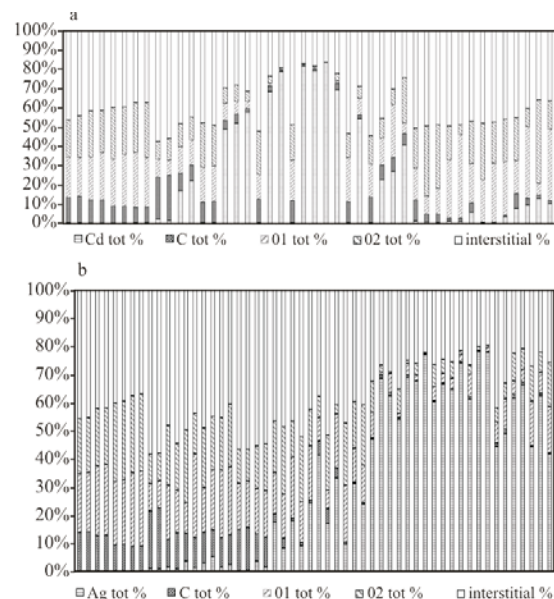
Fig. 6 Bands character calculated for a – cadmium and
b – silver oxalates, for highest symmetry point Γ

small amount of carbon and oxygen electrons. Thus, de-spite the evident similarities between both DOS-es (the mainly between respective carbon and oxygen atoms to-tal DOS-es), we cannot consider this as the confirmation of the similar thermal decomposition of these compounds.

On Figs 5a and b the calculated band structures for cadmium and silver oxalates are shown. Due to the number of electrons and thus number of bands, especially for silver oxalate, detailed analysis exceeds the scope of this paper and will be published elsewhere. Nevertheless it is worth to mention here, that both band structures show similarities, as one could expect, taking into account that in both structures we have cations with

filled d-electron shells, weakly interacting with surrounding oxygen atoms located at almost uniform distances from these cations and well defined oxalate groups. The characters of individual band change not only from band to band, but also for different k-point (different directions in reciprocal lattice), so detailed analysis is omitted here, but some insight can be obtained from the analysis of band characters for most symmetric k point i.e. Γ point. On Figs 6a and b, such characters are presented in the form of cumulative histograms, where each band is represented by one bar filled with percentage number of electrons from

Table 2 Electron density properties in bond critical points calculated for cadmium and silver oxalates

		Dist. from atom 1/Å	Dist. from atom 2/Å	Bond length/Å	$\nabla^2\rho(r)$/Å^{-5}	$\rho(r)$/e Å^{-3}
$Ag_2C_2O_4$						
r_1	Ag_1–O_1^{ii}	1.1944	1.0917	2.2861	5.6100	0.3864
r_2	Ag_1–O_1^{iii}	1.3346	1.2166	2.5512	3.0220	0.2130
r_3	Ag_1–O_2^{ii}	1.1753	1.0705	2.2458	6.2900	0.4170
r_4	Ag_1–O_2^{iii}	1.2917	1.1795	2.4712	3.6680	0.2520
r_5	C_1–O_1^{i}	0.4165	0.8139	1.2304	−10.5050	2.7257
r_6	C_1–O_2^{ii}	0.4207	0.8202	1.2409	−11.4980	2.6528
r_7	C_1–C_3	0.7975	0.7975	1.5950	−11.3440	1.5217
CdC_2O_4						
r_1	Cd–O_1	1.1631	1.0790	2.2421	6.1740	0.4324
r_2	Cd–O_2^{i}	1.2018	1.1192	2.3210	5.0030	0.3608
r_3	Cd–O_2^{ii}	1.2171	1.1298	2.3469	4.6630	0.3344
r_4	C_1–O_1	0.4239	0.8223	1.2462	−13.8280	2.6474
r_5	C_1–O_2^{i}	0.4302	0.8340	1.2642	−14.4960	2.5327
r_6	C_1–C_2	0.7790	0.7790	1.5580	−14.1200	1.6635

individual atoms adding up to 100% (with delocalized electrons off the bands). Such approach is complementary to the DOS picture and it is clearly visible, that both structures show similar behavior – there are few bands dominated by metal d-electron, with small participation of oxygen electrons and the dominating rest of the bands, where the electrons from oxygen are mixed with those from carbon.

The electron density distribution data obtained from SCF calculations where used in Bader's QTAiM analysis of electron density topology. In Table 2, the results of these calculations are presented. The values of calculated total charges (on a base of unit cell partitioning scheme proposed by Bader) are presented on Figs 1 and 2. It is interesting to notice, that such analysis provide very useful information about the properties of electron density at bond critical points, which can be easily connected with bonds properties. The results presented in Table 2 show again, this time in real space (as opposite to reciprocal space in case of band structure) that the structures under consideration are qualitatively very similar: the values of electron density in BCP are largest for carbon–oxide bonds, next smaller for carbon–carbon bond and much smaller, but similar in metal–oxygen bonds, indicating that none of the latter bonds is distinguished.

Conclusions

The main purpose of undertaken studies, the results of which are presented here, was the attempt to apply theoretical methods of electronic structure calculations to analysis of the thermal decomposition process in anhydrous oxalates, which can follow different paths (e.g. metal+carbon dioxide, metal oxide+carbon oxide+carbon dioxide, metal carbonate+carbon oxide) even when the differences in chemical composition and properties of constituent atoms are small. This attempt is based on the assumption, that the results of the ab initio calculations of band structure and electron density topology can give an insight into the origins and chosen path of thermal decomposition process in given oxalate. As the first example we have taken cadmium and silver oxalates, due to their similar thermal decomposition path (both decompose to metal and carbon dioxide). The obtained results show that indeed such theoretical analysis can be used as an additional tool for both the explanation and the prediction of the thermal decomposition reaction path and its products types. The detailed analysis of the results of electronic structure calculations in conjunction with the calculated bond orders and bond valences, carried from the point of view of the thermal decomposition, will be presented in the second part of this paper [23].

References

1 Y. D. Kondrashev, V. S. Bogdanov, S. N. Golubev and G. F. Pron, Zh. Struct. Khim, 26 (1985) 90.
2 E. Jeanneau, N. Audebrand and D. Louer, Acta Cryst., C57 (2001) 1012.
3 D. Y. Naumov, N. V. Podberezkaya, E. V. Boldyreva and A. V. Virovets, J. Struct. Chem., 37 (1996) 480.
4 B. Małecka, E. Drożdż-Cieśla and A. Małecki, Thermochim. Acta, 423 (2004) 13.
5 B. Małecka, E. Drożdż-Cieśla and A. Małecki, J. Therm. Anal. Cal., 68 (2002) 819.
6 M. E. Brown, D. Dollimore and A. K. Galwey, Comprehensive Chemical Kinetics, Vol. 22. Reactions In Solid State, C. H. Bamford, C. F. H. Tipper Eds., Elsevier, Amsterdam 1980.
7 A. K. Galwey and M. E. Brown, J. Therm. Anal. Cal., 90 (2007) 9.
8 V. V. Boldyrev, I. S. Nevyantsev, Y. I. Mikhailov and E. F. Khayretdinov, Kinet. Katal., 11 (1970) 367.
9 H. J. Borchardt and F. Daniels, J. Am. Chem. Soc., 79 (1957) 41.
10 B. S. Randhawa and M. Kaur, J. Therm. Anal. Cal., 89 (2007) 251-255.
11 D. Dollimore, Thermochim. Acta, 117 (1987) 331.
12 S. Rane, H. Uskaikar, R. Pednekar and R. Mhalsikar, J. Therm. Anal. Cal., 90 (2007) 627.
13 J. Fujita, K. Nakamoto and M. Kobayashi, J. Phys. Chem., 61 (1957) 1014.
14 P. Blaha, K. Schwarz, G. K. H. Madsen, D. Kvasnicka and J. Luitz, WIEN2k, An Augmented Plane Wave+Local Orbitals Program for Calculating Crystal Properties (Karlheinz Schwarz, Techn. Universität Wien, Austria), ISBN 3-9501031-1-2, (2001).
15 J. C. Slater, Phys. Rev., 51 (1937) 151.
16 T. L. Loucks, Augmented Plane Wave Method, Benjamin, NewYork 1967.
17 O. K. Andersen, Solid State Commun., 13 (1973) 133.
18 D. R. Hamann, Phys. Rev. Lett., 42 (1979) 662.
19 E. Wimmer, H. Krakauer, M. Weinert and A. J. Freeman, Phys. Rev., B24 (1981) 864.
20 D. J. Singh, Planewaves, Pseudopotentials and the LAPW Method, Kluwer Academic Publishers, Dordrecht, 1994.
21 J. P. Perdew, K. Burke and M. Ernzerhof, Phys. Rev. Lett., 77 (1996) 3865.
22 D. Y. Naumov, A. V. Virovets, N. V. Podberezkaya and E. V. Boldyreva, Acta Cryst., C51 (1995) 60.
23 A. Koleżyński and A. Małecki, J. Therm. Anal. Cal., (accepted).